Lawrence Berkeley National Laboratory
LBL Publications

Title
3D numerical simulation of a deepwater EM exploration survey

Permalink
https://escholarship.org/uc/item/9084962g

Authors
Hoversten, G. Michael
Newman, Gregory A.
Geier, Nathan
et al.

Publication Date
2004-03-31

3D numerical simulation of a deepwater EM exploration survey

G. Michael Hoversten*, Gregory A. Newman, Lawrence Berkeley National Laboratory, Nathan Geier, Guy Flanagan, ConocoPhillips

Summary

An analysis of a current offshore prospect has been carried out using three-dimensional numerical modeling of a controlled source electromagnetic (CSEM) exploration system. The analysis considers the sensitivity of data presentations to assumptions about the background model. The numerical simulations show that false anomalies and significant distortion to anomaly magnitude can be caused by normalization of the observed electric fields by fields calculated from an incorrect or oversimplified background model. Bathymetry effects on the measured electric fields can, if not accounted for, produce anomalies as large as those of target sands. Good background models can be constructed by taking advantage of the magnetotelluric data recorded by marine receivers during times when the CSEM transmitter is not in operation.

Introduction

Developments over the last decade in the application of marine electromagnetic systems in petroleum exploration were driven first by the need for structural information in areas where high velocity materials such as salt or basalt covered prospective sediments. Both CSEM and passive source magnetotelluric (MT) systems were considered for petroleum related exploration (Hoversten et al. 1994). It was noted from the beginning that CSEM systems have superior resolving capabilities when compared to MT, but the logistics of deployment and ease of data interpretation favored MT, resulting in a preponderance of work on marine MT systems (Hoversten et al. 1998, Constable et al. 1998, Hoversten et al. 2000). The development of CSEM systems actually predates the marine MT systems where CSEM was used for crustal investigations in the deep oceans (Fillaux 1987, Constable & Cox 1996). In the last few years, attention has been focused on the use of CSEM systems in direct detection/mapping of hydrocarbon (Ellingsrud et al. 2002).

A marine CSEM system consists of a ship towed electric dipole source and a number of seafloor deployed recording instruments capable of recording orthogonal electric (and optionally magnetic) fields. A common configuration is described by Ellingsrud et al. (2002) where the electric dipole transmitter length is on the order of 100m and is towed in a neutrally buoyant configuration approximately 50m off the seafloor to avoid bathymetry changes as well as collision with stationary receiver systems. An electric current waveform is sent into the transmitter at a variable fundamental frequency between 0.01 and 1 Hz. The response is measured at the array of receivers on the seafloor. Marine CSEM systems have progressed from academic instruments in the 1980's to second generation commercial systems in the 1990's and may now be termed "third-generation" and are operated by at least four commercial contractors in Europe and the USA.

We have carried out three dimensional (3D) numerical simulations of marine CSEM data over a potential deepwater exploration prospect. This scenario is representative of a number of commercial marine CSEM acquisitions which have been carried out in recent years and are planned in the near future. The location and structure of the target sands are well characterized by seismic data. The question to be answered is; where do the sands contain high hydrocarbon saturation and where do they contain high water saturation? The presence of small amounts of gas complicates the interpretation of seismic AVO anomalies to the point that standard interpretation for fluid content is unreliable. AVO analysis in the area has a demonstrated inability to accurately predict the hydrocarbon to water ratio. This has lead to the consideration of marine CSEM as a method for distinguishing predominantly hydrocarbon versus predominately water saturated sands.

Theory and Method

The electrical resistivity of reservoir rocks is highly sensitive to water saturation, varying by several orders of magnitude over the range of water saturation. In sedimentary marine environments brine saturated sediments typically range between 0.5 and 2 ohm-m (Ωm). In contrast, hydrocarbon saturated sediments range between 100 and 1000 Ωm. It is this large contrast in resistivity that CSEM techniques exploit to distinguish hydrocarbon from brine saturated targets.

The model considered here consists of four large, well defined slope channel sand systems (denoted sands 1 – 4 in Figure 1) with average widths of 3 to 4 km and total vertical thickness between 100 and 200m. Each system is comprised of inter-bedded sand-shale sequences with a 30% net to gross. Log resistivities of hydrocarbon saturated sands range between 100-1000 Ωm. The average bulk resistivity of the sand sequences in the model was conservatively chosen to be 30 Ωm based on the net-to-gross and a lower end hydrocarbon saturation resistivity of 100 Ωm. A 3D background model was constructed by generating three synthetic resistivity logs using existing regional logs as a guide. The three synthetic logs had different resistivity vs. depth trends in the range 0.5 to 2.0 Ωm from seafloor to 5km below sea floor (BSF). The synthetic logs were interpolated in 3D using a minimum-curvature algorithm to produce a laterally and vertically variable background. In addition, the first layer of cells below the seafloor interface had a Gaussian variation of 50% about 1 Ωm to simulate possible near surface variations due to unknown

conditions such as seepage induced carbonate build up. The bathymetry changes by 700m over the prospect (shallower at +y and deeper at –y in Figure 1) and plays a significant role in the measured response. A 3D staggered-grid finite difference (FD) algorithm (Newman & Alumbaugh 1997) was used to simulate the electric fields measured on the seafloor from 100m electric dipole transmitters operating at 0.25 Hz located 50m above the seafloor.

Due to limitations of computer resources two FD grids were used, a coarse 190 x 200 x 150 mesh with cell sizes of 200 x 200 x 100 m in x, y and z respectively and a fine mesh of 270 x 300 x 280 with cell sizes of 150 x 150 x 50 in x, y and z. Lateral conductivity jumps either from seafloor variations or from bathymetry changes produce electric field jumps from FD node to node which can be manifested as site-to-site jitter in the calculated responses using the coarse mesh. Effects of this can be seen in the normalized responses shown in Figure 2. The coarse grid required 2 hour run times per transmitter using 27 CPU's (average clock speed 1.4 GHz) of a PC Linux cluster. The fine grid calculations required 0.5 hours per transmitter using 1000 CPU's on an IBM SP cluster. Fine grid calculations were used sparingly to; 1) verify the elimination of grid noise
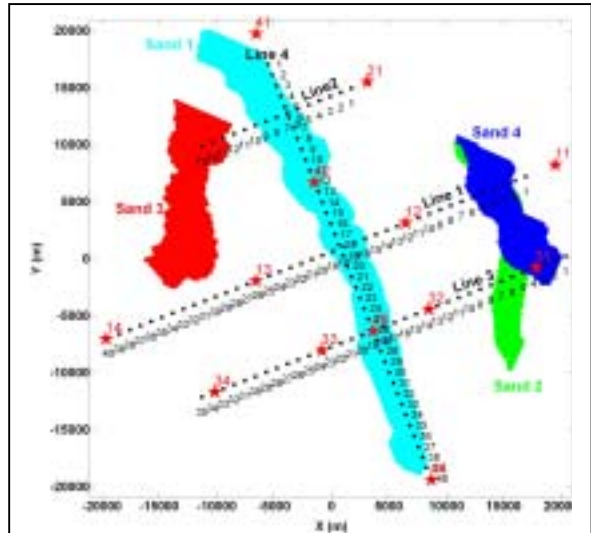

Figure 1. Sand channels. Red stars are CSEM transmitter positions, dipole sources oriented parallel to receiver lines. Black dots are E field receiver positions.

associated with sea floor bathymetry at finer meshing, 2) to verify that the coarse grid results jitter about the true solution in areas with rapid bathometric change and, 3) to verify that coarse grids calculations carried all the correct response characteristics of the sands and bathymetry. Modeling without bathymetry requires cells to be on the order of 1/3 a skin depth (δ) in the seawater, where $\delta = \sqrt{\rho/f} * 503$ m, ρ is resistivity and f is frequency. In the presence of bathymetry cell sizes must be reduced to at least 1/4 δ to eliminate grid noise.

A common data representation is to normalize the observed electric field amplitude (E) by a background response and plot the results as a function of distance from the transmitter. Observed E increases over resistive areas (hydrocarbon saturated) due to the increased current density above the resistor caused by exclusion of current from the resistor. While the use of normalization produces a readily interpreted data presentation with minimal compute requirements, the process can significantly bias the results if incorrect background fields are used. Figure 2 shows E as a function of distance from transmitter 31 located on line 3 (Figure 1). A flat seafloor with water depth at transmitter 31 is used. Three different normalizations are shown; 1) a layered
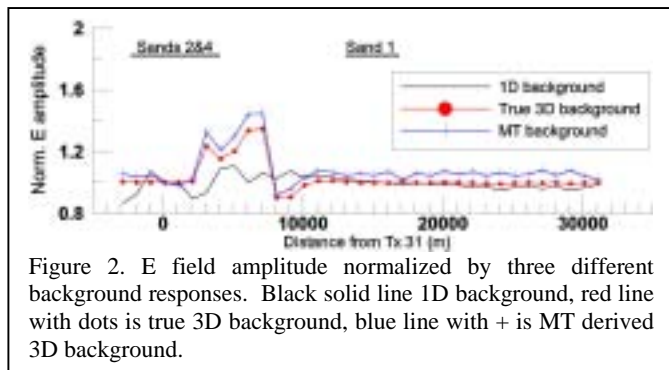

Figure 2. E field amplitude normalized by three different background responses. Black solid line 1D background, red line with dots is true 3D background, blue line with + is MT derived 3D background.

(1D) model with 1 Ωm sediment, 2) the true laterally and vertically variable background and, 3) a 3D background derived from three two-dimensional (2D) MT inversions followed interpolation to 3D (to be discussed below). Sands 2&4 are stacked with the top of sand 4 1.3km BSF and the base of sand 2 1.7 km BSF. The top of sand 3 is 2km BSF, with its base 2.2km BSF. The maximum anomaly occurs at offsets that corresponds to approximately 6 δ in the background material. This translates to the maximum anomaly between 5-7 km in Figure 2 at 0.25 Hz in 1 Ωm sediment. The anomaly is shifted to far offsets away from the actual location of the sands. The shift of the anomaly is dependent on the relative location between source and target, and decreases as the source becomes more distant from the target. Sand 1 which is between 13 and 18 km offsets from the transmitter does not produce an anomaly because it is too distant from the transmitter.

Figure 3 shows calculated E field amplitude (used to produce normalized plots such as those shown in Figures 2 and 4 from transmitter 32 as a function of offset. The anomaly from transmitter 31 over sands 2 & 4 (Figure 2) is 50% above the background response. The anomaly from transmitter 32 over the deeper and thinner sand 1 is 20%, (Figure 3). Given current technology both of these anomalies should be observable in the field, although a 20% anomaly is probably near the limit of what can be distinguished in the presence of instrument noise and un-accounted for geologic variation.

The bathymetry affects both the background and target response. As the seawater layer thins with progressively larger offset in Figure 3 the current density in the seawater increases to try to keep the total current constant, this increases the E fields at the receivers. The 1D background model does not account for the increase in E, this can be seen at offsets greater than 10 km in the

blow up section of Figure 3. Normalizing by the 1D response causes the ratio of observed/background to increase. This means that unaccounted for changes in bathymetry such as ridges, or slopes can produce false anomalies if observations are normalized by 1D model responses. The interaction between bathymetry and the target is more complex. Figure 3 shows that the background response at short offsets is identical between models with bathymetry and a flat seafloor, whereas the 3D response with the sand bodies is magnified in the case with bathymetry included. This means that the bathymetry effects at far offset are redistributing currents at depth (where the sands are located).

Figures 2 and 3 illustrate the need for an accurate background model if normalized E is to be reliably interpreted for indications of resistive (hydrocarbon bearing) sands. One way to produce a reasonable background model is to make use of the data acquired by the receivers while the CSEM transmitter is not in operation. The receivers acquire the natural magnetotelluric (MT) signals throughout their deployment. This data can be processed and interpreted using 2D or even 3D inversion. To illustrate this, three cross sections, oblique to line 3, were extracted from the 3D EM model (including the sands) near the beginning, middle and end of the line. These were used to generate 2D MT data in the frequency range 0.001 to 2 Hz, which was inverted to produce 2D resistivity models that fit the observed MT data to within 5%. It should be noted that no indication of the sands is seen in the MT inverted resistivity sections, as is well known thin resistive layers are essentially invisible to MT. These three inverted MT sections were then interpolated using a minimum-curvature algorithm to produce a 3D background model. The MT derived model was used to calculate the CSEM background response used for normalization and denoted "MT background" in Figure 2. We see that in general the MT derived background model reproduces the true anomalies well. However, over sands 2&4 from transmitter 32 (not shown) the MT
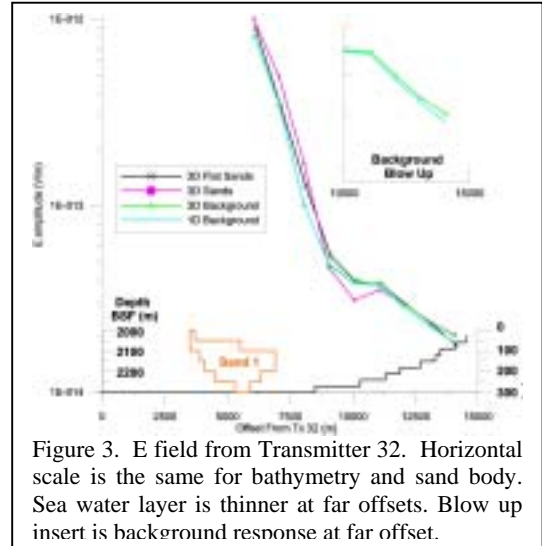

Figure 3. E field from Transmitter 32. Horizontal scale is the same for bathymetry and sand body. Sea water layer is thinner at far offsets. Blow up insert is background response at far offset.

background anomaly is larger than the true anomaly. We speculate that this is due to differences between the true background and the 3D interpolated MT models in this vicinity.

A key exploration question is the location of potential hydrocarbon-water contacts within sand channel systems. To address this, the resistivity of sand 1 was changed from 30 Ωm to 1 Ωm (brine saturated sand) below Y= -10,000 m (Figure 1), representing a hydrocarbon-water contact. Figure 4a shows E normalized by the true background along line 3 where Sand 1 is truncated 1.5 km in –Y from the line. The reduction in the sand 1 anomaly is only about 10% and could not reliably be interpreted as an off-line hydrocarbon-water contact given all other noise sources. Figure 4b shows the response on line 4, which runs along the length and over the center of sand 1. To either side of the transmitter there are approximately equal magnitude anomalies in the 4-9 km offset range. The Figure 4b response represents the sensitivity function of this source-receiver configuration, since the target, to first order, is unchanging in either direction. When the sand is truncated at ~ +2km from transmitter 43 the anomaly disappears. Profiling along the sand channels provides the best way to detect lateral changes in hydrocarbon-water ratios within the sand system.
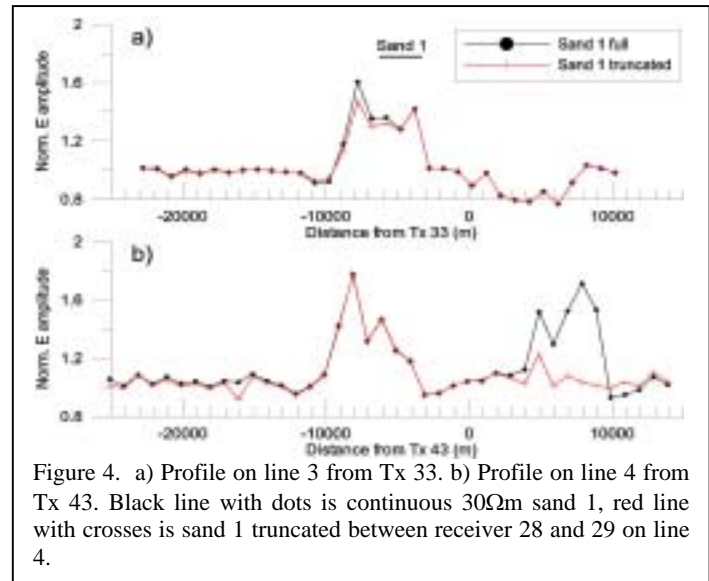

Figure 4. a) Profile on line 3 from Tx 33. b) Profile on line 4 from Tx 43. Black line with dots is continuous 30Ωm sand 1, red line with crosses is sand 1 truncated between receiver 28 and 29 on line 4.

Another survey configuration that should be considered is to position receivers on a regular grid with the transmitter flown above the receiver array in such a way that the data can be sorted into constant source-receiver offset. The optimum offset is dependent of the background resistivity and target depths but for most marine environments it will be between 5 and 10 km. Figure 5 shows E normalized by the true background for an offset of 5.5km. The constant offset anomaly is largest, reaching 1.8, over the shallow sections of sand 3. The anomalies also reach 1.8 over the area where sands 2 and 4 are stacked. As sand 2 extends to –Y out from under sand 4 the anomaly drops to 1.2. The shallowest part of sand 1 (top at 2km below seafloor) is beneath the maximum 1.4 anomaly. The sand deepens in either direction reaching a depth of 3 km below seafloor near Y=-15000. These

data were simulated using the fine mesh with 143 transmitters and 1440 receivers on a regular grid over the model. In practice such data can be acquired using the principal of reciprocity which allows the interchange of the source and receiver locations. Thus 143 receiver deployments could be used in conjunction with 1440 transmitter locations to generate the data. The generation of 1440 transmitter locations is easily done if the source is towed on a regular line interval over the prospect.

Conclusions

The simulations carried out for this prospect are representative of many situations where CSEM data can be used for determining hydrocarbon saturation of prospective sands. The anomalies seen are large, reaching nearly 100% and are of the order of 20% over sands at depths of 3km below seafloor. The presentation of the data as observed E normalized by a calculated background response can produce significant error and even false anomalies if over simplified models are used. In particular, if seafloor bathymetry changes significantly over the prospect, 3D modeling of the bathymetry will probably be required for proper normalization. If the sediment resistivity varies laterally within normal ranges (0.5–2 Ωm) use of a 1D background model can produce significant error. However, in such circumstances a good background model can be constructed by using MT inversion of data acquired during CSEM transmitter down time.

This work considers only the presentation of normalized E field for simple interpretation. This type of data can be quantitatively interpreted for hydrocarbon saturation given good seismic constraints on structure by forward modeling different scenarios once a reasonable 3D background model has been derived. A

Figure 5. Noramlized Ex for source-receiver separation of 5.5km. Data is plotted at source-receiver midpoint.

more rigorous, and computationally demanding, approach is to use full 2D or 3D inversion of the field data. This subject is covered in a 2004 SEG companion paper, "Large scale 3D inverse electromagnetic modeling for reservoir characterization" (Newman & Hoversten, 2004).
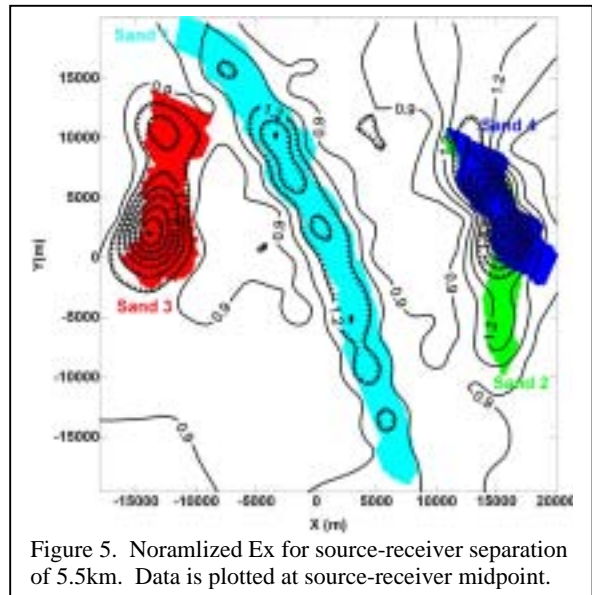
References

Constable, S., Orange, A., Hoversten, G. M., Morrison, H.F., 1998, Marine Magnetotellurics for petroleum Exploration Part 1: A seafloor equipment system: Geophysics, **63**, 816-825.

Constable, S., and C., S., Cox, 1996, Marine controlled source electromagnetic sounding 2. The PEGASUS experiment: J. Geophys. Res., **101**, 5519-5530

Ellingsrud, S., Eidesmo, T., Johansen, S., Sinha, M.C., MacGregor, L. M., Constable, S., 2002, Remote sensing of hydrocarbon layers by seabed logging (SBL): Results from a cruise offshore Angola: The Leading Edge, **21**, 972-982

Fillux. J. H., 1987, Instrumentation and experimental methods for oceanic studies, Geomagnetism, Ed. Jacobs, J. A, Acad. Press, Orlando, FL, USA, 143-248.

Hoversten, G. M., Unsworth, Martyn , 1994, SubSalt Imaging via Seaborne Electromagnetics, Offshore Technology Conference, Houston, TX. Vol. **26**, Vol. 1 p. 231-240.

Hoversten, G. M., Morrison, H.F., Constable, S., 1998, Marine Magnetotellurics for Petroleum Exploration Part 2: Numerical analysis of subsalt resolution: Geophysics, **63**, 826-840.

Hoversten, G. M., Constable, S. C., Morrison, H. F., 2000, Marine Magnetotellurics for Base Salt Mapping: Gulf of Mexico Field Test at the Gemini Structure: Geophysics, **65**, 1476-1488.

Hoversten, G., M., Gritto, R., Washbourne, J., Daley, T., M.., 2003, Pressure and Fluid Saturation Prediction in a Multicomponent Reservoir, using Combined Seismic and Electromagnetic Imaging: Geophysics, **68**, 1580-1591.

Newman, G. A. and Alumbaugh, D. L., 1997, Three-dimensional massively parallel electromagnetifc inversion – I. Theory: Geophys. J. Int., **128**, 345-354.

Newman, G. A., Hoversten, G. M., 2000, Solution strategies for two- and three-dimensional electromagnetic inverse problems: Inverse Problems, **16**, 1357-1375.

Newman, G. A., Hoversten, G. M., 2004, Large scale 3D inverse electromagnetic modeling for reservoir characterization: SEG Denver, 2004.

3D Numerical simulation of marine EM survey